Nuclear Instruments and Methods in Physics Research A 783 (2015) 110–116

Contents lists available at ScienceDirect

Nuclear Instruments and Methods in Physics Research A

journal homepage: www.elsevier.com/locate/nima

# Modeling and characterization of X-ray yield in a polychromatic, lab-scale, X-ray computed tomography system

J.C.E. Mertens, Nikhilesh Chawla*

*Materials Science and Engineering, Arizona State University Tempe, AZ 85287-5604, USA*

ARTICLE INFO

*Article history:*
Received 3 December 2014
Received in revised form
22 January 2015
Accepted 19 February 2015
Available online 26 February 2015

*Keywords:*
Polychromatic
Bremsstrahlung
X-ray
Detection
Micro-tomography
Micro-CT

ABSTRACT

A modular X-ray computed micro-tomography (μXCT) system is characterized in terms of X-ray yield resulting both from the generated X-ray spectrum and from X-ray detection with an energy-sensitive detector. The X-ray computed tomography system is composed of a commercially available cone-beam microfocus X-ray source and a modular optically-coupled-CCD-scintillator X-ray detector. The X-ray yield is measured and reported in units independent from exposure time, X-ray tube beam target current, and cone-beam-to-detector geometry. The polychromatic X-ray source is modeled as a broad Bremsstrahlung X-ray spectrum in order to understand the effect of the controllable parameters, that is, X-ray tube accelerating voltage and X-ray beam filtering. An approach is adopted which expresses the absolute number of emitted X-rays. The response of the energy-sensitive detector to the modeled spectrum is modeled as a function of scintillator composition and thickness. The detection efficiency model for the polychromatic X-ray detector considers the response of the light collection system and the electronic imaging array in order to predict absolute count yield under the studied conditions. The modeling approach is applied to the specific hardware implemented in the current μXCT system. The model's predictions for absolute detection rate are in reasonable agreement with measured values under a range of conditions applied to the system for X-ray microtomography imaging, particularly for the LuAG:Ce scintillator material.

## 1. Introduction

In X-ray imaging, it is desirable to have both a high signal rate and high imaging resolution. In the low X-ray flux environment of cone-beam, lab-scale imaging, the importance of X-ray detection efficiency is particularly important [1]. In microfocus X-ray tubes, the X-ray power is inversely proportional to the spatial resolution (in l p/mm), that is, the spatial resolution typically decreases (gets worse) with increasing X-ray signal [2,3]. On the X-ray detector side, a similar situation is realized, particularly for the case of a thin scintillator screen lens-coupled to a digital (CCD) detector configuration [4], as employed in the μXCT system used in the current study [5–7]. Simply put, thicker scintillator screens have higher absorption efficiency and thus produce higher ultimate detected signal. However, the increased thickness also decreases the detector's spatial resolution.

Previous researchers have shown the utility of custom built detectors as well as complete lab-scale CT instruments and have provided insight to many modeling approaches in the design process [3–10]. Recently, a fully customized lab-scale X-ray computed micro-tomography (μXCT) instrument implementing a commercially available microfocus X-ray source and a lens-coupled CCD-to-scintillator X-ray detector for performing micrometer-scale imaging of material systems has been constructed, and is leveraged in the current study to explore several imaging factors which dictate performance [6,7]. Clearly, a compromise is needed between the detected signal rate and the spatial resolution from control over both the X-ray generation mechanisms (accelerating voltage and target current/power) and the X-ray detection mechanisms (scintillator composition and thickness). Presently, a new approach to modeling the energy-sensitive detector's interaction with the polychromatic X-ray source is provided. The modeling methods are detailed and the modeling predictions are compared with measured values for a specific system. The characterization of the imaging parameters' effect on spatial resolution is beyond the scope of the present work, although it is required for a full understanding of the competition between spatial resolution and X-ray yield. This study aims to elucidate and quantify the imaging system's detection yield as a function of various controllable parameters for the X-ray computed tomography system with the understanding that the spatial resolution is typically inversely affected.

## 2. Performance expectations from modeling

### 2.1. Modeling X-ray detection efficiency

Factors influencing the detection efficiency of the X-ray detector were investigated by modeling the X-ray energy dependence of

---

* Corresponding author.
*E-mail address:* nchawla@asu.edu (N. Chawla).

http://dx.doi.org/10.1016/j.nima.2015.02.040
0168-9002/

scintillators with varying thickness and the wavelength sensitive transfer efficiency of an optical system and electronic sensor in response to varying scintillated wavelengths. The X-ray detector used in the system was a modular scintillator-lens-mirror-CCD-camera tandem, and has been previously described in detail [5–7]. The CCD incorporated in the detector was the back-illuminated e2v CCD230-42 (in the Apogee Imaging Alta U230). The mid-band (visible sensitive) CCD chip produces digital counts in response to light in the optical range. The efficiency of the CCD sensor varies depending on the wavelength. The number of photons of a particular wavelength that are detected out of the total number of photons is a metric of detector efficiency. The detector's design had three critical components which controlled detection efficiency: the scintillator, the optical system, and the CCD. The optical system and the CCD had efficiency functions which depended on the wavelength of light being transferred or detected. For the components in series, the product of the individual components' transfer efficiency was used to describe the detector's optical efficiency, $\eta_{optical}(\lambda)$, as

$$\eta_{optical}(\lambda) = \eta_{CCD}(\lambda) * \eta_{window}(\lambda) * \eta_{mirror}(\lambda) * \eta_{lens}(\lambda) \tag{1}$$

where $\eta_{lens}(\lambda)$ is the transfer efficiency of the lens, $\eta_{mirror}(\lambda)$ is the transfer efficiency of optical light of the right-angle mirror, and $\eta_{window}(\lambda)$ is the efficiency of the $MgF_2$ CCD window, and $\eta_{CCD}(\lambda)$ is the CCD's quantum efficiency, all as a function of wavelength. The calculated resulting effective efficiency for the optical/CCD detector as a function of wavelength, from Eq. (1), is plotted as the solid blue line in Fig. 1 using manufacturer data for the components used in this system's optical detector. The overall shape of the curve was a result of $\eta_{CCD}(\lambda)$, as the other loss functions were relatively negligible. The sharp edges in the curve were a result of efficiency data of limited wavelength range for the other optical components. Between the sharp edges, the reduction was a result of optical losses considered for the mirror, lens, and CCD window.

The effective scintillated-light-to-digital-counts conversion efficiency, $\eta_{\lambda/e}$, for three candidate scintillators as calculated in conjunction with the detailed optical light detector (Fig. 1) is summarized in Table 1. The scintillated-light-to-digital-counts conversion efficiency was approximated based on the optical transfer efficiency spectrum of the detector at the wavelength of maximum scintillation intensity, using the following equation:

$$\eta_{\lambda/e} \approx \eta_{optical}(\lambda(I_{scint}^{max})). \tag{2}$$

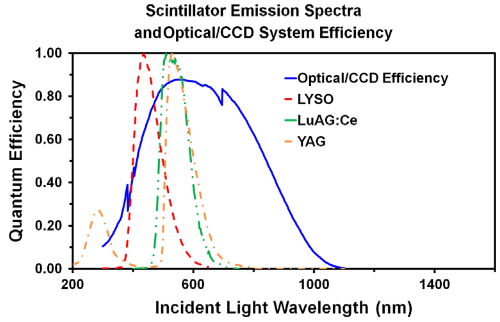

**Fig. 1.** The relative emission spectra of three scintillation materials (*y*-axis not shown) of relatively good fit with the detector efficiency for the CCD/optical system at various light wavelengths. (For interpretation of the references to color in this figure, the reader is referred to the web version of this article.)

**Table 1**
The effective X-ray to optical light conversion efficiency, $\eta_{\lambda/e}$, calculated for various scintillator materials. The value can be visualized by the optical efficiency at the wavelength of scintillator peak emission from the curves shown in Fig. 1.

| Scintillator | $\eta_{\lambda/e}$ at Peak emission, calculated for optical/CCD system |
|---|---|
| LuAG:Ce | 0.855 |
| YAG | 0.872 |
| LYSO | 0.628 |

While Table 1 provides a reasonable estimate of the relative emission spectra, the absolute emission of each scintillator was also considered in order to get an absolute comparison of the detectors' efficiency when coupled. This was computed by considering the light yield for each scintillator material. Also, the absorption efficiency of the scintillator must be considered [4]. Further, the light collection efficiency of the lens as a result of the numeric aperture must be considered [4]. Following Koch et al. [4], these factors were modeled with the following relation:

$$DQE = \frac{SNR_{OUT}^2}{SNR_{IN}^2} = \eta_{abs}(E^x)\left(1 + \frac{1 + 1/\eta_{\lambda/e}}{\eta_{coll} * (E^x/E^\lambda)\eta_{x/\lambda}}\right)^{-1} \tag{3}$$

where *DQE* is the detection efficiency, $\eta_{abs}(E^x)$ is the absorption efficiency at an X-ray energy, $E^x$, $\eta_{\lambda/e}$ is the light to electron conversion efficiency of the detector, $\eta_{coll}$ is the light collection efficiency of the lens based on the numeric aperture and the scintillator index of refraction, $\eta_{x/\lambda}$ is the effective X-ray to optical light conversion efficiency, and $E^\lambda$ is the energy of the optical light being detected by the CCD. The light to electron conversion efficiency is the solid blue line in Fig. 1 which is based on all losses in the conversion of optical light to electronic signal, but not considering the amount of light entering the system as a function of numeric aperture or light source. The collection efficiency is expressed as a function of the numeric aperture, *NA*, and the index of refraction of the scintillator, *n* [4]

$$\eta_{coll} = (NA/n)^2/4. \tag{4}$$

The index of refraction for select scintillators is provided in Table 2. A high numeric aperture produces high light collection efficiency. The amount of light collected by the lens is also dependent on the X-ray absorption efficiency of the scintillator [4]. It can be seen in Eq. (3) that high absorption efficiency is desired. This is a function of thickness. As seen in Eq. (3), the absorption efficiency, $\eta_{abs}$, is also a function of X-ray energy, because it is a function of the photoelectric absorption coefficient, $-\mu_{photo}/\rho(E^x)$. The absorption efficiency $\eta_{abs}(E^x)$, is written as:

$$\eta_{abs}(E^x) = 1 - I/I_0 = 1 - e^{(-\mu_{photo}/\rho * \rho * t)} \tag{5}$$

where $I_0$ is the initial X-ray intensity, $I$ is the transmitted intensity as a function of X-ray energy, $\rho$ is the density of the scintillator, and $t$ is the thickness of the scintillator. The photoelectric absorption coefficients of the scintillators were calculated using the NIST X-COM calculator [11], and the total absorption was calculated for a scintillator compositions and thicknesses over the energy range of interest. The density of selected scintillators is provided in Table 2.

By assuming that the energy of light emitted by the scintillator is equal to the energy of the maximum output intensity, the light yield of the scintillator material, *LY*, in units of photons/energy of

**Table 2**
Physical properties for various scintillator materials, including index of refraction, light yield, peak emission wavelength, and density. [12–14].

| | ***LYSO*** | ***LuAG:Ce*** | ***YAG*** | ***CsI:Tl*** |
|---|---|---|---|---|
| **Index of refraction, *n*** | 1.81 | 1.85 | 1.82 | 1.80 |
| **Light Yield, *LY* (photons/keV X-ray)** | 32 | 20 | 40 | 65 |
| **Peak wavelength (nm)** | 420 | 535 | 550 | 540 |
| **Density, $\rho$(g/cm³)** | 7.1 | 6.73 | 4.57 | 4.52 |